Application of Common Midpoint Gathers to Medical Pulse-Echo Ultrasound for Optimal Coherence and Improved Sound Speed Estimation in Layered Media

Rehman Ali
Department of Electrical Engineering
Stanford University
Stanford, CA
rali8@stanford.edu

Dongwoon Hyun
Department of Radiology
Stanford School of Medicine
Stanford, CA
dongwoon.hyun@stanford.edu

Jeremy J. Dahl
Department of Radiology
Stanford School of Medicine
Stanford, CA
jjdahl@stanford.edu

***Abstract*—In seismic imaging, common midpoint (CMP) gathers are collections of time-series data organized by source-receiver pairs having a common midpoint. CMP gathers have been used in geophysics to image the subsurface of the Earth and estimate wave velocity as a function of depth. According to the Van Cittert-Zernike (VCZ) theorem, if the signals from a CMP gather are focused using an ideal set of delays based on the true speed of sound in the medium, there should be a perfect correlation between any two signals in the CMP gather in the absence of noise. In ultrasound imaging, Walker et al. have applied this concept to translating transmit and receive apertures. The goal of this work is to apply CMP gathers to pulse-echo ultrasound imaging in order to improve coherence-based sound speed estimation in layered media.**

***Index Terms*—Shot-Gather Migration, Medical Ultrasound Imaging, Adjoint-Based Method**

I. Introduction and Background

Sound speed estimation in medical pulse-echo ultrasound imaging is growing area of research. Many advancements have been made in obtaining accurate estimates of the speed of sound in the medium. Currently, there are two broad classes of sound speed estimators applied in medical ultrasound imaging. The first set of methods reconstruct the speed of sound in a medium by accounting for differential times of flight between different ray paths [1], [2]. These differential times of flight enable tomographic reconstruction of the speed of sound in the medium. The tomographic method is primarily used to detect cancerous cysts due to their high speed of sound compared the rest of the medium. Another group of techniques assumes that the speed of sound in the medium only varies axially and applies layered medium models during sound speed reconstruction [3]–[5]. These layered medium-based approaches tend to yield highly-accurate sound speed estimates in media where sound speed changes with the layers of tissue being imaged. In particular, these sound speed estimators are primarily applied to liver imaging in order to estimate liver fat-fraction based on the sound speed in the liver.

Wave-velocity estimation in seismic imaging has followed a similar trajectory [6], [7]. The first velocity analysis techniques in seismic imaging assumed that wave velocity primarily varies with imaging depth but not laterally. This assumption was often appropriate because the Earth's subsurface can be understood as layers of rock with different wave velocities that generally increase with depth due to the compaction of each layer. However, there are many exceptions to this such as salt bodies, which can lead to large lateral changes in wave velocity. This problem has motivated tomographic techniques based on ray-tracing methods and waveform inversion techniques for estimating wave velocities in the medium.

Seismic and ultrasound imaging have tackled wave-velocity estimation in layered media using similar methods. Both approaches estimate an effective focusing velocity as a function of depth, and both approaches estimate the wave-velocity in each individual layer in the medium as a function of depth [8]. However, one key difference between the two sets of approaches is that the seismic imaging approach processes collected recordings using common-midpoint (CMP) gathers. A CMP gather collects all source-receiver pairs having a common midpoint, and applies focusing delays to each source-receiver pair having a common midpoint. The distance between the source and receiver is the offset. The signals in a common midpoint gather are typically plotted as a function of the half-offset and the zero-offset time, which corresponds to the imaging depth. The first stage of velocity analysis estimates the effective focusing velocity, or stacking velocity, at each depth by finding the focusing velocities that optimally align the signals at each depth, much like in ultrasound. However, the ultrasound-equivalent wave-velocity estimator acts in the imaging domain rather than the time-depth used in seismic imaging, and the ultrasound images are produced by using all sources and receivers available rather than first applying a CMP gather.

Although CMP gathers have not previously been applied

978-1-7281-5448-0/20/$31.00 ©2020 IEEE

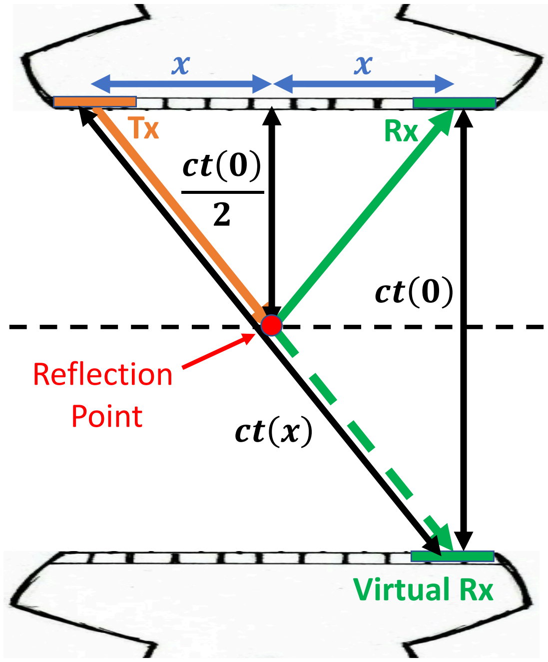

Fig. 1. Imaging Geometry for Common Midpoint Gathers. The half-offset between transmit and receive beam origins is x and speed of sound in the medium is c. The time it takes for sound from the transmit beam origin to be reach the reflection point and return to the receive origin is $t(x)$.

to sound speed estimation based on layered medium models, the idea behind the CMP gather has been used to estimate phase aberration. The ultrasound-equivalent to CMP gathers is known as the translating-transmit apertures (TTA) algorithm [9]–[11]. However, unlike the CMP gather of seismic imaging, which use point sources and receivers, the TTA algorithm uses an entire transmit and receive aperture. In the TTA algorithm, the transmit aperture is translated across the aperture as the corresponding receive aperture moves in the opposite direction, effectively maintaining a common midpoint. The main motivation behind this arrangement is that the point spread function (PSF) induced by each pair of transmit and receiver apertures, having a common midpoint, remains roughly constant as the apertures translates. Because the PSF remains roughly constant, the correlation between images produced by each pair of transmit and receive apertures should be very close to 1. This property of the PSF is then used to accurately estimate aberration delays on an element-wise basis. In this work, we exploit the same property of the PSF in TTA algorithm in order to estimate sound speed in layered media using the CMP-based model from seismic imaging.

II. Theory

A. Sound Speed Estimation in a CMP Gather

Figure 1 illustrates the geometry for a CMP gather with a transmit and a receive beam origin. Denote $t(x)$ as the travel time, required for sound from the transmit beam origin to reach the reflection point and return to the receive beam origin, as a function of the half-offset x between the transmit and receive beam origins. In terms of the zero-offset time $\tau = t(0)$ and sound speed c in the medium, the travel time $t(x)$ as a function of half-offset x is

$$t^2(x) = \tau^2 + \frac{4x^2}{c^2} \tag{1}$$

The effective focusing sound speed $c_{eff}(\tau)$ is determined as a function of τ by finding the sound speed c that maximizes the coherence factor (CF) [12] at each τ. Since τ is the zero-offset time, it effectively serves as measure of imaging depth. In the end, we have travel times as a function of τ and x:

$$t^2(x) = \tau^2 + \frac{4x^2}{c_{eff}^2(\tau)} \tag{2}$$

B. Kinematics of Wave-Velocity Estimation

Now we create new variables $t_H(x) = t(x)/2$ and $\tau_H = \tau/2$ which denote the one-way travel times from either beam origin to the reflection point. These one-way times obey the equation

$$t_H^2(x) = \tau_H^2 + \frac{x^2}{c_{eff}^2(\tau_H)} \tag{3}$$

We differentiate this travel-time equation with respect to x in order to obtain

$$2t_H \frac{dt_H}{dx} = \frac{2x}{c_{eff}^2(\tau_H)}, \tag{4}$$

which can be rearranged to obtain $c_{eff}(\tau_H)$ as

$$c_{eff}(\tau_H) = \sqrt{\frac{x/t_H}{dt_H/dx}}. \tag{5}$$

Recall that in a layered medium, Snell's law states that at an interface between two media with different sound speeds c_1 and c_2, the angles of the rays θ_1 and θ_2 must obey the equation

$$p = \frac{dt_H}{dx} = \frac{\sin\theta_1}{c_1} = \frac{\sin\theta_2}{c_2}, \tag{6}$$

where p is the conserved quantity known as the Snell parameter, which is also the lateral component of the slowness (reciprocal of sound speed) for this ray. The Snell parameter allows us to revise equation (5) as

$$c_{eff}(\tau_H) = \sqrt{\frac{x}{pt_H}}. \tag{7}$$

Now we consider sound that travels on a particular path in a layered medium. Denote $x(p, t_H)$ as the x-coordinate and and $\theta(p, t_H)$ as the angle of a ray of sound with Snell parameter p as a function of time t_H:

$$x(p, t_H) = \int_0^{t_H} c(p, t_H)\sin\theta(p, t_H)dt_H, \tag{8}$$

$$x(p, t_H) = p\int_0^{t_H} c^2(p, t_H)dt_H, \tag{9}$$

where $c(p, t_H)$ is the sound speed encountered along the ray path for Snell parameter p at time t_H. If we insert equation (9) into equation (7), we obtain a new equation for the effective focusing sound speed c_{eff} as a function of the true sound speed c in the medium.

$$c_{eff}(\tau_H) = \sqrt{\frac{1}{t_H}\int_0^{t_H} c^2(p, t_H) dt_H}. \tag{10}$$

To further simplify this equation, we consider the zero-offset path so that $t_H = \tau_H$ and $p = 0$ since the angle $\theta = 0$. Since c only varies as a function of depth in a layered medium, c can be understood to be be a function of τ_H, which increases monotonically with depth, so that

$$c_{eff}(\tau_H) = \sqrt{\frac{1}{\tau_H}\int_0^{\tau_H} c^2(\tau_H) d\tau_H}, \tag{11}$$

which is equivalent to

$$c_{eff}(\tau) = \sqrt{\frac{1}{\tau}\int_0^{\tau} c^2(\tau) d\tau}. \tag{12}$$

In seismic imaging, this effective focusing velocity is also known as root-mean-square (RMS) velocity because it represents the root-mean square of the true velocity in the medium as a function of the zero-offset time. Because refraction was taken into account during the derivation, this RMS velocity also takes into account any refraction due to the velocity changes in a layered medium.

C. Dix Inversion

Since $c_{eff}(\tau)$ is measured by CF maximization, the goal of this section is to invert the formula given in equation (12) to obtain $c(\tau)$. This inversion formula is known as Dix inversion [8], whose differential form is given here:

$$c(\tau) = \sqrt{\frac{d}{d\tau}\left(\tau c_{eff}^2(\tau)\right)}. \tag{13}$$

III. Methods

A. Simulations

Field II [13] was used to simulate the complete multistatic dataset for diffuse random scattering. The Field II simulation used a 128-element linear array with 0.154 mm pitch, and transmit pulse with 8 MHz center frequency and 70% fractional bandwidth. The sound speed in the medium is 1540 m/s and the sampling frequency of the channel data is 100 MHz. Another simulation was performed in k-Wave [14] for diffuse scattering in two-layer media where the sound speed is 1480 m/s over the first 15 mm of depth into the media and 1600 m/s over the remainder of the medium. All remaining simulation parameters such as the transducer configuration, and transmit pulse sequence are identical to the Field II simulation.

B. Phantom Experiment

A 1 cm porcine slab is placed on top of an ATS 549 phantom (1460 m/s) to create a medium with two layers having different sound speeds. Multistatic synthetic aperture channel data was captured using an L12-3v probe using a Verasonics Vantage 256 scanner.

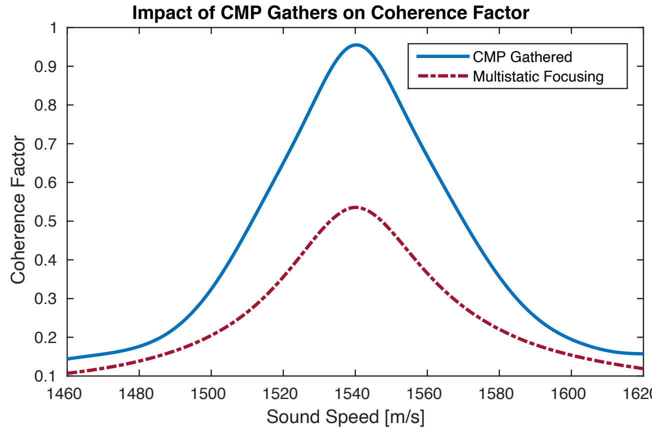

Fig. 2. Impact of CMP gathers on CF as a Focusing Metric for Sound Speed Estimation. The peak CF value at the true speed of sound in the medium (1540 m/s) is much closer to 1 as a result of CMP gathering the channel data.

C. Sound Speed Estimation

In each imaging case, an 16-element translating transmit aperture with a 16-element translating receive aperture were used to create the signals for a CMP gather. Maximization of CF was used to determine $c_{eff}(\tau)$ as a function of the zero-offset time τ. The resulting $c_{eff}(\tau)$ were smoothed prior to applying the Dix inversion formula (13) to reduce the impact of noise in the final estimate of $c(\tau)$.

IV. Results and Discussion

Figure 2 shows CF as a focusing metric for sound speed estimation when the channel data is conventionally focused using multistatic synthetic aperture (as in [3]) and after applying CMP gathers with the TTA algorithm. The peak CF value becomes much closer to 1 as a result of applying CMP gathers to the channel data. As shown in previous work [9]–[11], the main advantage of the TTA algorithm is to bring the correlation of receive channel data closer to 1 by maintaining a roughly constant PSF at the intended focus. We demonstrate the same changes in the CF as a focusing metric for sound speed estimation

Figure 3 demonstrates the complete sound speed estimation procedure in simulation for a two-layer medium. The top panel shows that the effective RMS velocity can be found by taking the peak of the CF at each depth (converted from zero-offset time to depth for ease of interpretation). Dix inversion is used in the bottom panel to obtain local estimates of the speed of sound as a function of depth. Figure 4 demonstrates the methodology in phantom experiments.

Despite increasing the peak CF value, there is relatively little improvement in the sound speed estimates themselves. This is ultimately because although the PSF is constant between each pair of transmit and receive apertures, they are all still equally affected by off-axis scattering in a diffuse scattering medium. The application of the TTA algorithm also imposes certain trade-offs on our ability to accurately estimate the speed of sound. For example, an increase in the size of the

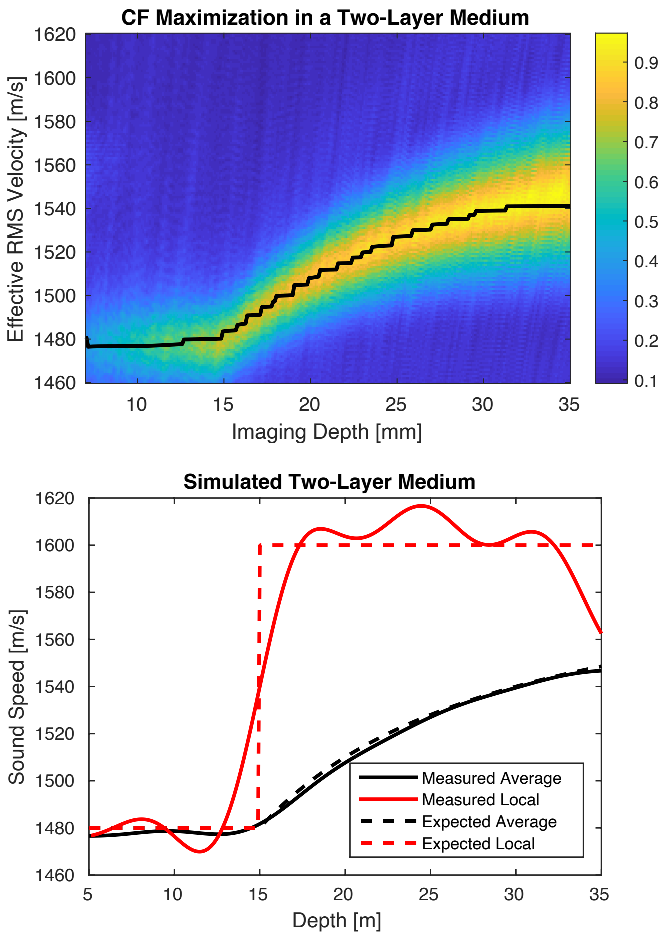

Fig. 3. Sound speed estimation in a simulated two-layer medium. The top panel shows the coherence as a function of depth and focusing sound speed. The effective RMS velocity follows the peak of the CF as a function of depth. The bottom panel shows the estimate of the local sound speed in the medium by Dix inversion.

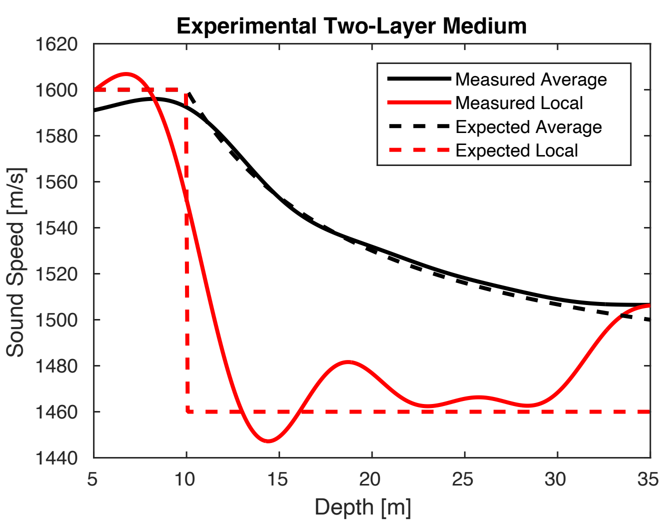

Fig. 4. Sound speed estimation in an experimental two-layer phantom. The estimated speed of sound in the porcine layer and ATS phantom materials are close to their reported values.

transmit and receive apertures causes a proportional increase in SNR for the beamformed ultrasound signals and limits off-axis scattering by tightening the PSF. However, increasing aperture sizes limits the total half-offset x, which can also reduce the accuracy of sound speed estimates. For this reason, too small or too large of a translating aperture also limits the accuracy of the sound speed estimates.

V. Conclusions and Future Work

In this work, we successfully adapt the concept of common-midpoint gathers from seismic imaging to medical ultrasound for sound speed estimation in layered media. We demonstrate that this approach maximizes the coherence of signals during the sound speed estimation process, and can be used to accurately determine the speed of sound as a function of depth in layered media.

Acknowledgment

Rehman Ali would like to thank the National Defense Science and Engineering Graduate (NDSEG) Fellowship for funding his graduate studies and research work.

References

[1] M. Jaeger, G. Held, S. Peeters, S. Preisser, M. Grünig, and M. Frenz, "Computed ultrasound tomography in echo mode for imaging speed of sound using pulse-echo sonography: proof of principle," *Ultrasound in medicine & biology*, vol. 41, no. 1, pp. 235–250, 2015.

[2] S. J. Sanabria, E. Ozkan, M. Rominger, and O. Goksel, "Spatial domain reconstruction for imaging speed-of-sound with pulse-echo ultrasound: simulation and in vivo study," *Physics in Medicine & Biology*, vol. 63, no. 21, p. 215015, 2018.

[3] R. Ali and J. J. Dahl, "Travel-time tomography for local sound speed reconstruction using average sound speeds," in *2019 IEEE International Ultrasonics Symposium (IUS)*. IEEE, 2019, pp. 2007–2010.

[4] M. Imbault, A. Faccinetto, B.-F. Osmanski, A. Tissier, T. Deffieux, J.-L. Gennisson, V. Vilgrain, and M. Tanter, "Robust sound speed estimation for ultrasound-based hepatic steatosis assessment," *Physics in Medicine & Biology*, vol. 62, no. 9, p. 3582, 2017.

[5] M. Imbault, M. D. Burgio, A. Faccinetto, M. Ronot, H. Bendjador, T. Deffieux, E. O. Triquet, P.-E. Rautou, L. Castera, J.-L. Gennisson *et al.*, "Ultrasonic fat fraction quantification using in vivo adaptive sound speed estimation," *Physics in Medicine & Biology*, vol. 63, no. 21, p. 215013, 2018.

[6] J. F. Claerbout and I. Green, "Basic earth imaging," 2008.

[7] B. L. Biondi, *3D seismic imaging*. Society of Exploration Geophysicists, 2006.

[8] C. H. Dix, "Seismic velocities from surface measurements," *Geophysics*, vol. 20, no. 1, pp. 68–86, 1955.

[9] W. F. Walker, "C-and d-weighted ultrasonic imaging using the translating apertures algorithm," *IEEE transactions on ultrasonics, ferroelectrics, and frequency control*, vol. 48, no. 2, pp. 452–461, 2001.

[10] G. Ng, W. Walker, and G. Trahey, "Improvement of signal correlation for adaptive imaging using the translating transmit aperture algorithm," in *1996 IEEE Ultrasonics Symposium. Proceedings*, vol. 2. IEEE, 1996, pp. 1395–1400.

[11] G. C. Ng, P. D. Freiburger, W. F. Walker, and G. E. Trahey, "A speckle target adaptive imaging technique in the presence of distributed aberrations," *IEEE transactions on ultrasonics, ferroelectrics, and frequency control*, vol. 44, no. 1, pp. 140–151, 1997.

[12] P.-C. Li and M.-L. Li, "Adaptive imaging using the generalized coherence factor," *IEEE transactions on ultrasonics, ferroelectrics, and frequency control*, vol. 50, no. 2, pp. 128–141, 2003.

[13] J. A. Jensen, "Field: A program for simulating ultrasound systems," in *10TH NORDICBALTIC CONFERENCE ON BIOMEDICAL IMAGING, VOL. 4, SUPPLEMENT 1, PART 1: 351–353*. Citeseer, 1996.

[14] B. E. Treeby and B. T. Cox, "k-wave: Matlab toolbox for the simulation and reconstruction of photoacoustic wave fields," *Journal of biomedical optics*, vol. 15, no. 2, p. 021314, 2010.